PERGAMON

International Journal of Hydrogen Energy 25 (2000) 1185–1203

International Journal of HYDROGEN ENERGY

www.elsevier.com/locate/ijhydene

Synthesis and characterization of potassium iodo hydride

Randell L. Mills *, Bala Dhandapani, Nelson Greenig, Jiliang He

BlackLight Power, Inc., 493 Old Trenton Road, Cranbury, NJ 08512, USA

Abstract

A novel inorganic hydride compound KHI which comprises a high binding energy hydride ion was synthesized by reaction of atomic hydrogen with potassium metal and potassium iodide. Potassium iodo hydride was identified by time-of-flight secondary ion mass spectroscopy, X-ray photoelectron spectroscopy, ^{1}H and ^{39}K nuclear magnetic resonance spectroscopy, Fourier transform infrared spectroscopy, electrospray ionization time-of-flight mass spectroscopy, liquid chromatography/mass spectroscopy, thermal decomposition with analysis by gas chromatography, and mass spectroscopy, and elemental analysis. Hydride ions with increased binding energies may form many novel compounds with broad applications.

1. Introduction

Intense extreme ultraviolet (EUV) emission was observed at low temperatures (e.g. $< 10^3$ K) from atomic hydrogen and certain atomized elements or gaseous ions which ionize at integer multiples of the potential energy of atomic hydrogen [1–6]. Based on its exceptional emission, we used potassium metal as a catalyst to release energy from atomic hydrogen. Mills [7] predicts an exothermic reaction whereby certain atoms or ions serve as catalysts to release energy from hydrogen to produce an increased binding energy hydrogen atom called a hydrino having a binding energy of

$$\text{Binding energy} = \frac{13.6 \text{ eV}}{(1/p)^2}, \tag{1}$$

where p is an integer greater than 1, designated as $H[a_H/p]$ where a_H is the radius of the hydrogen atom. Hydrinos are predicted to form by reacting an ordinary hydrogen atom with a catalyst having a net enthalpy of reaction of about

$$m \cdot 27.2 \text{ eV}, \tag{2}$$

where m is an integer. This catalysis releases energy from the hydrogen atom with a commensurate decrease in size of the hydrogen atom, $r_n = na_H$. For example, the catalysis of $H(n = 1)$ to $H(n = \frac{1}{2})$ releases 40.8 eV, and the hydrogen radius decreases from a_H to $\frac{1}{2}a_H$.

A catalytic system is provided by the ionization of t electrons from an atom each to a continuum energy level such that the sum of the ionization energies of the t electrons is approximately mX 27.2 eV where m is an integer. One such catalytic system involves potassium. The first, second, and third ionization energies of potassium are 4.34066, 31.63, 45.806 eV, respectively [8]. The triple ionization ($t = 3$) reaction of K to K^{3+}, then, has a net enthalpy of reaction of 81.7426 eV, which is equivalent to $m = 3$ in Eq. (2).

$$81.7426 \text{ eV} + K(m) + H\left[\frac{a_H}{p}\right] \rightarrow K^{3+} + 3e^- + H\left[\frac{a_H}{(p+3)}\right] + [(p+3)^2 - p^2]X13.6 \text{ eV}, \tag{3}$$

$$K^{3+} + 3e^- \rightarrow K(m) + 81.7426 \text{ eV}. \tag{4}$$

The overall reaction is

$$H\left[\frac{a_H}{p}\right] \rightarrow H\left[\frac{a_H}{(p+3)}\right] + [(p+3)^2 - p^2]X13.6 \text{ eV}. \tag{5}$$

Potassium ions can also provide a net enthalpy of a multiple of that of the potential energy of the hydrogen atom.

* Corresponding author. Tel.: +001-609-490-1040; fax: +001-609-490-1066.

E-mail address: rmills@blacklightpower.com (R.L. Mills).

0360-3199/00/$20.00
PII: S0360-3199(00)00037-9

The second ionization energy of potassium is 31.63 eV; and K^+ releases 4.34 eV when it is reduced to K. The combination of reactions K^+ to K^{2+} and K^+ to K, then, has a net enthalpy of reaction of 27.28 eV, which is equivalent to $m = 1$ in Eq. (2).

$$27.28 \text{ eV} + K^+ + K^+ + H\left[\frac{a_H}{p}\right] \rightarrow K + K^{2+} + H\left[\frac{a_H}{(p+1)}\right] + [(p+1)^2 - p^2]X13.6 \text{ eV}, \quad (6)$$

$$K + K^{2+} \rightarrow K^+ + K^+ + 27.28 \text{ eV}. \quad (7)$$

The overall reaction is

$$H\left[\frac{a_H}{p}\right] \rightarrow H\left[\frac{a_H}{(p+1)}\right] + [(p+1)^2 - p^2]X13.6 \text{ eV}. \quad (8)$$

A novel hydride ion having extraordinary chemical properties given by Mills [7] is predicted to form by the reaction of an electron with a hydrino (Eq. (9)). The resulting hydride ion is referred to as a hydrino hydride ion, designated as $H^-(1/p)$.

$$H\left[\frac{a_H}{p}\right] + e^- \rightarrow H^-(1/p). \quad (9)$$

The hydrino hydride ion is distinguished from an ordinary hydride ion having a binding energy of 0.8 eV. The latter is hereafter referred to as "ordinary hydride ion". The hydrino hydride ion is predicted [7] to comprise a hydrogen nucleus and two indistinguishable electrons at a binding energy according to the following formula:

$$\text{Binding energy} = \frac{\hbar^2\sqrt{s(s+1)}}{8\mu_e a_0^2[(1+\sqrt{s(s+1)})/p]^2} - \frac{\pi\mu_0 e^2\hbar^2}{m_e^2 a_0^3}\left(1+\frac{2^2}{[(1+\sqrt{s(s+1)})/p]^3}\right), \quad (10)$$

where p is an integer greater than one, $s = \frac{1}{2}$, π is pi, $\hbar$ is Planck's constant bar, μ_0 is the permeability of vacuum, m_e is the mass of the electron, μ_e is the reduced electron mass, a_0 is the Bohr radius, and e is the elementary charge. The ionic radius is

$$r_1 = \frac{a_0}{p}(1+\sqrt{s(s+1)}); \; s = \frac{1}{2}. \quad (11)$$

From Eq. (11), the radius of the hydrino hydride ion $H^-(1/p)$; p = integer is $1/p$ that of ordinary hydride ion, $H^-(1/1)$.

A novel inorganic hydride compound KHI which comprises high binding energy hydride ions was synthesized by reaction of atomic hydrogen with potassium metal and potassium iodide. Potassium iodo hydride was identified by time-of-flight secondary ion mass spectroscopy (ToF-SIMS), X-ray photoelectron spectroscopy (XPS), ^1H and ^{39}K nuclear magnetic resonance spectroscopy (NMR), Fourier transform infrared (FTIR) spectroscopy, electrospray ionization time-of-flight mass spectroscopy (ESITOFMS), liquid chromatography/mass spectroscopy (LC/MS), thermal decomposition with analysis by gas chromatography (GC), and mass spectroscopy (MS), and elemental analysis.

Alkali and alkaline earth hydrides react violently with water to release hydrogen gas which subsequently ignites due to the exothermic reaction with water. Typically metal hydrides decompose upon heating at a temperature well below the melting point of the parent metal. These saline hydrides, so called because of their salt-like or ionic character, are the monohydrides of the alkali metals and the dihydrides of the alkaline-earth metals. Mills predicts a hydrogen-type molecule having a first binding energy of about

$$\text{Binding energy} = \frac{15.5}{(1/p)^2} \text{ eV}. \quad (12)$$

Dihydrino molecules may be produced by the thermal decomposition of hydrino hydride ions. $H^-(\frac{1}{2})$ may be less reactive and more thermally stable than ordinary potassium hydride, but may react at high temperature to form a hydrogen-type molecule. Potassium iodo hydride $KH(\frac{1}{2})I$ may be heated to release dihydrino by thermal decomposition.

$$2KH(1/2)I \xrightarrow{\Delta} H_2^*\left[2c' = \frac{a_0}{\sqrt{2}}\right] + 2KI, \quad (13)$$

where $2c'$ is the internuclear distance and a_0 is the Bohr radius [7]. The possibility of releasing dihydrino by thermally decomposing potassium iodo hydride with identification by gas chromatography was explored.

The first ionization energy, IP_1, of the dihydrino molecule

$$H_2^*\left[2c' = \frac{\sqrt{2}a_0}{2}\right] \rightarrow H_2^*[2c' = a_0]^+ + e^- \quad (14)$$

is $IP_1 = 62$ eV ($p = 2$ in Eq. (12)); whereas, the first ionization energy of ordinary molecular hydrogen, $H_2[2c' = \sqrt{2}a_0]$, is 15.46 eV. Thus, the possibility of using mass spectroscopy to discriminate $H_2[2c' = \sqrt{2}a_0]$ from $H_2^*[2c' = a_0/\sqrt{2}]$ on the basis of the large difference between the ionization energies of the two species was explored. A novel high binding energy hydrogen molecule assigned to dihydrino $H_2^*[2c' = a_0/\sqrt{2}]$ was identified by the thermal decomposition of KHI with analysis by gas chromatography, and mass spectroscopy.

2. Experimental

2.1. Synthesis

Potassium iodo hydride was prepared in a stainless-steel gas cell shown in Fig. 1 comprising a Ti screen hydrogen

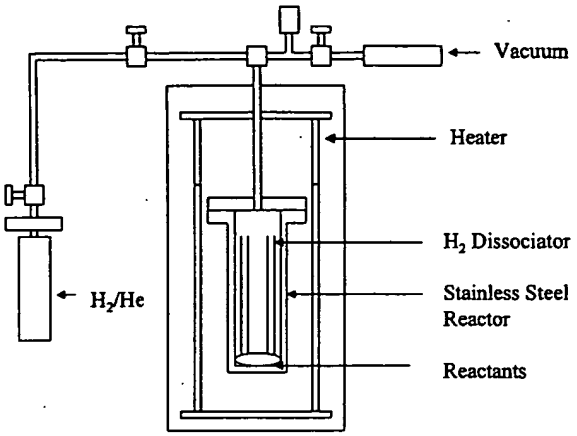

Fig. 1. Stainless-steel gas cell.

dissociator (Belleville Wire Cloth Co., Inc.), potassium metal catalyst (Aldrich Chemical Company), and KI (Aldrich Chemical Company 99.9%) as the reactant. The 304-stainless-steel cell was in the form of a tube having an internal cavity of 359 mm in length and 73 mm in diameter. The top end of the cell was welded to a high-vacuum 4 5/8 in bored through conflat flange. The mating blank conflat flange contained a single coaxial hole in which was welded a 3/8 in diameter stainless-steel tube that was 100 cm in length and contained an inner coaxial tube of $\frac{1}{8}$ in diameter. A silver-plated copper gasket was placed between the two flanges. The two flanges are held together with 10 circumferential bolts. The bottom of the $\frac{3}{8}$ in tube was flush with the bottom surface of the top flange. The outer tube served as a vacuum line from the cell and the inner tube served as a hydrogen or helium supply line to the cell. The cell was surrounded by four heaters. Concentric to the heaters was high-temperature insulation (AL 30 Zircar). Each of the four heaters were individually thermostatically controlled.

The cylindrical wall of the cell was lined with two layers of Ti screen totaling 150 g. 75 g of crystalline KI was poured into the cell. About 0.5 g of potassium metal was added to the cell under an argon atmosphere. The cell was then continuously evacuated with a high-vacuum turbo pump to reach 50 mtorr measured by a pressure gauge (Varian Convector, Pirrani type). The cell was heated by supplying power to the heaters. The heater power of the largest heater was measured using a wattmeter (Clarke -Hess model 259). The temperature of the cell was measured with a type K thermocouple (Omega). The cell temperature was then slowly increased over 2 h to 300°C using the heaters that were controlled by a type 97 000 controller. The power to the largest heater and the cell temperature and pressure were continuously recorded by a DAS. The vacuum pump valve was closed. Hydrogen was slowly added to maintain a pressure within the range of 1000–1500 torr. The temperature of the cell was then slowly increased to 650°C over 5 h. The hydrogen valve was closed except to maintain the pressure at 1500 torr. After 24 h, the temperature of the cell was reduced to 400°C at a rate of 15°C/h. The hydrogen supply was switched to helium which was flowed through the inner supply line to the cell while a vacuum was pulled on the outer vacuum line to remove volatilized potassium metal at 400°C. The cell was then cooled and opened. About 75 g of blue crystals were observed to have formed in the bottom of the cell.

The synthesis was repeated with the exception that the hydrogen was slowly added to maintain a pressure within the range of 1–10 torr. About 75 g of green crystals were observed to have formed in the bottom of the cell.

2.2. ToF-SIMS characterization

The crystalline samples were sprinkled onto the surface of a double-sided adhesive tape and characterized using a Physical Electronics TFS-2000 ToF-SIMS instrument. The primary ion gun utilized a $^{69}Ga^+$ liquid metal source. In order to remove surface contaminants and expose a fresh surface, the samples were sputter cleaned for 30 s using a 40 μm × 40 μm raster. The aperture setting was 3, and the ion current was 600 pA resulting in a total ion dose of 10^{15} ions/cm^2.

During acquisition, the ion gun was operated using a bunched (pulse width 4 ns bunched to 1 ns) 15 kV beam [9,10]. The total ion dose was 10^{12} ions/cm^2. Charge neutralization was active, and the post accelerating voltage was 8000 V. Three different regions on each sample of (12 μm)^2, (18 μm)^2, and (25 μm)^2 were analyzed. The positive and negative SIMS spectra were acquired. Representative post sputtering data are reported.

2.3. XPS characterization

A series of XPS analyses were made on the crystalline samples using a Scienta 300 XPS Spectrometer. The fixed analyzer transmission mode and the sweep acquisition mode were used. The step energy in the survey scan was 0.5 eV, and the step energy in the high-resolution scan was 0.15 eV. In the survey scan, the time per step was 0.4 s, and the number of sweeps was 4. In the high-resolution scan, the time per step was 0.3 s, and the number of sweeps was 30. C 1s at 284.5 eV was used as the internal standard.

The binding energies and features of core level electrons of control KI and the blue and green crystals comprising the alkali halido hydride KHI were analyzed by XPS. XPS analysis was conducted on a Kratos XSAM-800 spectrometer using nonmonochromatic Al K α (1468.6 eV) radiation. Samples were crushed in a glove box under argon and mounted on an analysis stub with copper tape. A piece of gold foil was stuck into the sample for calibration. The samples were transferred under an inert atmosphere. A survey spectrum was run from 1000 to 0 eV. For quantitative analysis, high-resolution spectra were run on core level electrons of interest, K 2p and I 3d electrons. A high-resolution

spectrum of the low binding energy region was also run from 100 to 0 eV that corresponded to the survey spectrum. Fixed analyzer transmission (FAT) mode was used in all measurements. For the survey scan, a pass energy of 320 eV was employed. A pass energy of 40 eV was used for high-resolution scans. In the cases where a charging effect was observed, the spectrum was corrected by using a calibration of the effect with the Au $4f_{7/2}$ peak at 84.0 eV as a first standard and the C 1s peak at 284.6 eV as a second standard.

2.4. NMR spectroscopy

^{1}H MAS NMR was performed on the blue crystals. The data were recorded on a Bruker DSX-400 spectrometer at 400.13 MHz. Samples were packed in zirconia rotors and sealed with airtight O-ring caps under an inert atmosphere. The MAS frequency was 4.5 kHz. During data acquisition, the sweep width was 60.06 kHz; the dwell time was 8.325 μs, and the acquisition time was 0.03415 s/scan. The number of scans was typically 32 or 64. Chemical shifts were referenced to external tetramethylsilane (TMS). The reference comprised KH (Aldrich Chemical Company 99%).

^{39}K MAS NMR was performed on the blue crystals. The data were recorded on a Bruker DSX-400 spectrometer at 18.67 MHz. Samples were packed in zirconia rotors and sealed with airtight O-ring caps under an inert atmosphere. The MAS frequency was 4.5 kHz. During data acquisition, the sweep width was 125 kHz; the dwell time was 4.0 μs, and the acquisition time was 0.01643 s/scan. The number of scans was 96. Chemical shifts were referenced to external KBr (Aldrich Chemical Company 99.99%). References comprised KI (Aldrich Chemical Company 99.99%) and the KH.

^{1}H MAS NMR was performed on the green crystals. The data were obtained on a custom built spectrometer operating with a Nicolet 1280 computer. Final pulse generation was from a tuned Henry radio amplifier. The ^{1}H NMR frequency was 270.6196 MHz. A 5 μs pulse corresponding to a 41° pulse length and a 3 s recycle delay were used. The window was ±20 kHz. The spin speed was 4.0 kHz. The number of scans was 600. The offset was 1541.6 Hz, and the magnetic flux was 6.357 T. The samples were handled under a nitrogen atmosphere. Chemical shifts were referenced to external tetramethylsilane (TMS). The reference comprised KH (Aldrich Chemical Company 99%) and equivalent molar mixtures of KH (Aldrich Chemical Company 99%) and KI (Aldrich Chemical Company 99.99%) prepared in a glove box under argon.

2.5. FTIR spectroscopy

Samples were transferred to an infrared transmitting substrate and analyzed by FTIR spectroscopy using a Nicolet Magna 550 FTIR Spectrometer with a NicPlan FTIR microscope. The number of scans was 250 for both the sample and background. The resolution was 8.000/cm. A dry air purge was applied.

2.6. Electrospray-ionization-time-of-flight-mass-spectroscopy (ESITOFMS)

The data were obtained on a Mariner ESI TOF system fitted with a standard electrospray interface. The samples were submitted via a syringe injection system (250 μl) with a flow rate of 5.0 μl/min. The solvent was water/ethanol (1 : 1). A reference comprised KI (Aldrich Chemical Company 99.99%).

2.7. Liquid-chromatography/mass-spectroscopy (LC/MS)

Reverse phase partition chromatography was performed with a PE Sciex API 365 LC/MS/MS System. The column was a LC C18 column, 5.0 μm, 150 × 2 mm (Columbus 100 Å Serial #207679). 31.1 mg of blue crystals were dissolved in 6.2 ml solvent of 90% HPLC water and 10% HPLC methanol to give a concentration of 5 mg/ml. The sample was eluted using a gradient technique with the eluents of a solution A (water + 5 mM ammonium acetate + 1% formic acid) and a solution B (acetonitrile/water(90/10) + 5 mM ammonium acetate + 0.1% formic acid). The gradient profile was

Time (min):	0	3	18	27	28	30
%A	100	100	0	0	100	Stop
%B	0	0	100	100	0	Stop

The flow rate was 1 ml/min. The injection volume was 1μl. The pump pressure was 110 psi.

A turbo electrospray ionization (ESI) and triple-quadrapole mass spectrometer was used. The turbo ESI converts the mobile phase to a fine mist of ions. These ions are then separated according to mass in a quadrapole radio frequency electric field. LC/MS provides information comprising (1) the solute polarity based on the retention time, (2) quantitative information comprising the concentration based on the chromatogram peak area, and (3) compound identification based on the mass spectrum or mass to charge ratio of a peak. The mass spectroscopy mode was positive. The selected ion mass to charge ratios (SIM) were $m/e = 39.0, 204.8, 370.6, 536.8$, and 702.6. The dwell time was 400 ms, and the pause was 2 ms. The turbo gas was 8 l/min (25 psi).

The controls comprised KI (Aldrich Chemical Company 99.99%) and sample solvent alone.

2.8. Elemental analysis

Elemental analysis was performed by Galbraith Laboratories, Inc., Knoxville, TN. Potassium was determined by Inductively Coupled Plasma using an ICP Optima 3000. Iodide

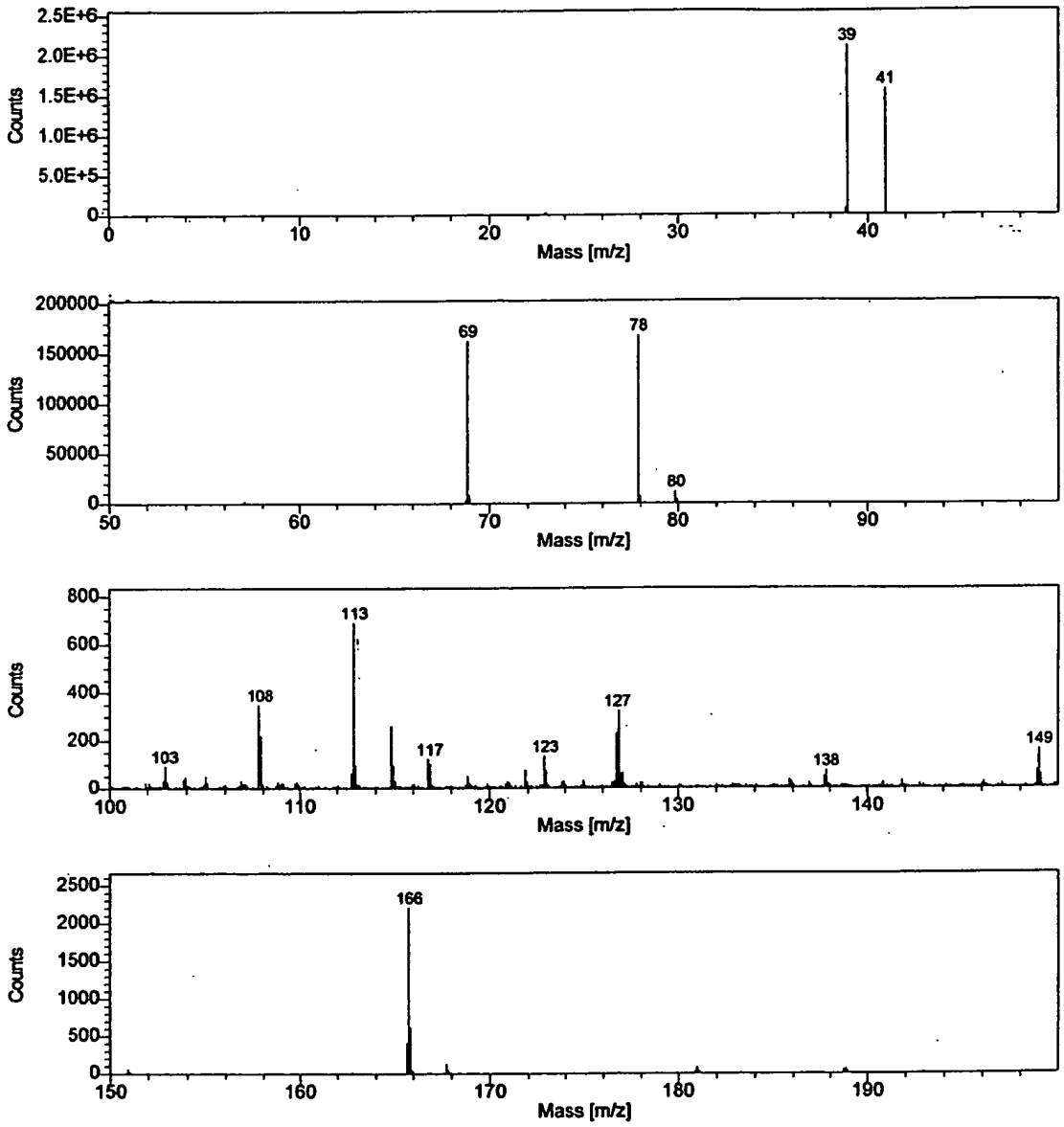

Fig. 2. The positive ToF-SIMS spectrum ($m/e = 0$–200) of the blue crystals.

was determined volumetrically by iodometric titration with thiosulfate. The hydrogen was determined by a Perkin-Elmer elemental analyzer (#240) using ASTM D-5291 method wherein the sample was combusted in a tube furnace at 950°C and the water was measured by a thermal conductivity detector. The sample was handled in an inert atmosphere.

2.9. Thermal decomposition with analysis by gas chromatography

The gas cell sample comprised deep blue crystals that changed to white crystals upon exposure to air over about a two week period. 0.5 g of the sample was placed in a thermal decomposition reactor under an argon atmosphere. The reactor comprised a 1/4″ OD by 3″ long quartz tube that was sealed at one end and connected at the open end with Swagelock™ fittings to a T. One end of the T was connected to a needle valve and a Welch Duo Seal model 1402 mechanical vacuum pump. The other end was attached to a septum port. The apparatus was evacuated to between 25 and 50 mtorr. The needle valve was closed to form a gas tight reactor. The sample was heated in the evacuated quartz chamber containing the sample with an external Nichrome wire heater using a Variac transformer. The sample was heated

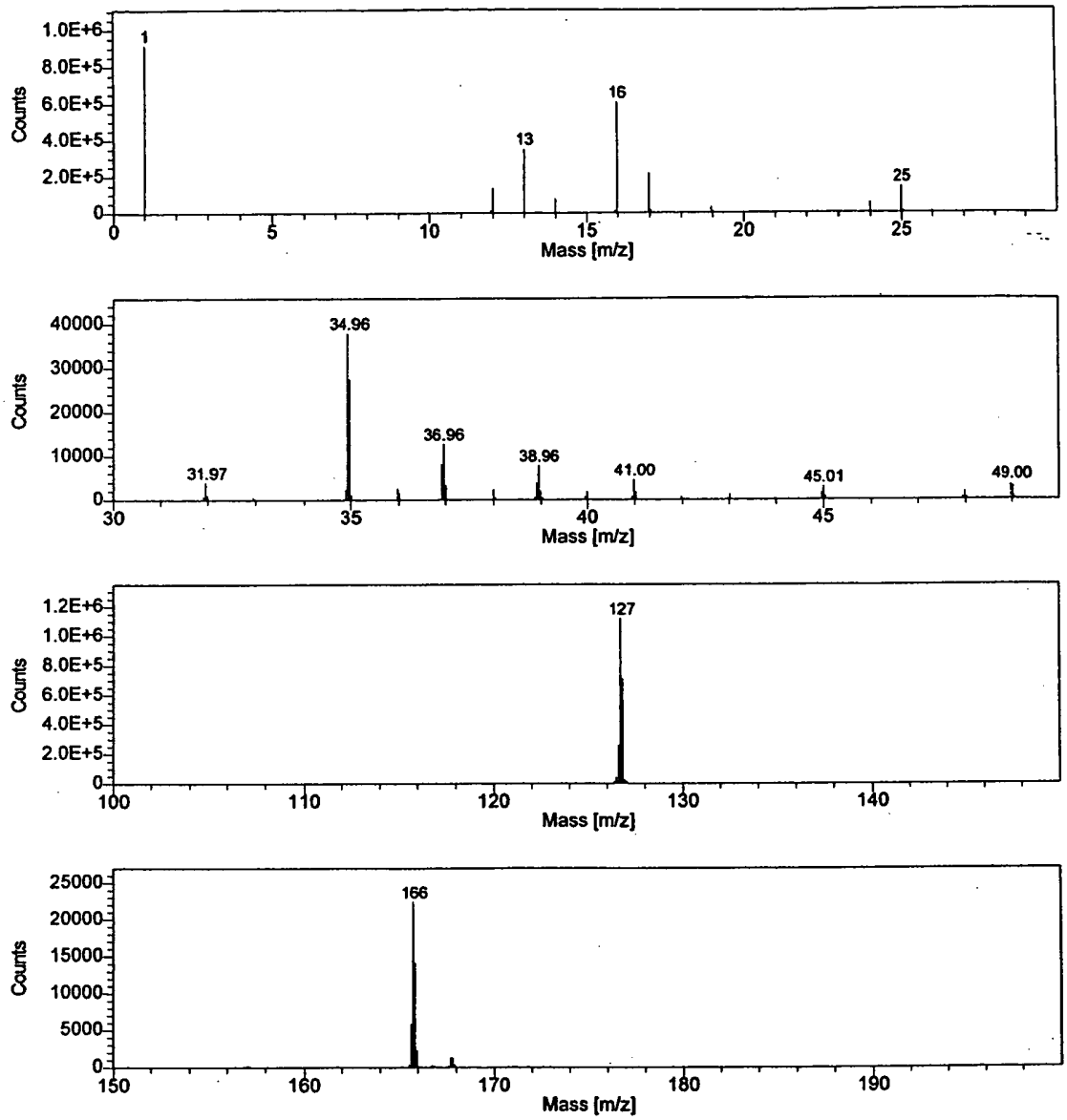

Fig. 3. The negative ToF-SIMS spectrum (m/e = 0–200) of the blue crystals.

to above 600°C by varying the transformer voltage supplied to the Nichrome heater until the sample melted. Gas released from the sample was collected with a 500 μl gas tight syringe through the septum port and immediately injected into the gas chromatograph. The reactor was cooled to room temperature, and a mixture of white and orange crystalline solid remained.

Gas samples were analyzed with a Hewlett Packard 5890 Series II gas chromatograph equipped with a thermal conductivity detector and a 60 m, 0.32 mm ID fused silica Rt-Alumina capillary PLOT column (Restek, Bellefonte, PA). The column was conditioned at 200°C for 18–72 h before each series of runs. Samples were run at −196°C using Ne as the carrier gas. The 60 m column was run with the carrier gas at 3.4 psi with the following flow rates: carrier — 2.0 ml/min, auxiliary — 3.4 ml/min, and reference — 3.5 ml/min, for a total flow rate of 8.9 ml/min. The split rate was 10.0 ml/min.

The control hydrogen gas was of ultrahigh purity (MG Industries). Control KI (Aldrich Chemical Company ACS grade, 99^{+}%,) was also treated by the same method as the blue crystals.

2.10. Thermal decomposition with analysis by mass spectroscopy

Mass spectroscopy was performed on the gases released from the thermal decomposition of the blue crystals. One end of a 4 mm ID fritted capillary tube containing about 5 mg of sample was sealed with a 0.25 in. Swagelock union and plug (Swagelock Co., Solon, OH). The other end was connected directly to the sampling port of a Dycor System 1000 quadrapole mass spectrometer (Model D200MP, Ametek, Inc., Pittsburgh, PA with a HOVAC Dri-2 Turbo 60 vacuum system). The capillary was heated with a Nichrome wire heater wrapped around the capillary. The mass spectrum was obtained at the ionization energy of 70 and 30 eV at different sample temperatures in the region $m/e = 0$–50. With the detection of hydrogen indicated by a $m/e = 2$ peak, the intensity as a function of time for masses $m/e = 1, 2, 4$, and 5 was obtained while changing the ionization potential (IP) of the mass spectrometer from 30 to 70 eV.

The control hydrogen gas was of ultrahigh purity (MG Industries).

3. Results and discussion

3.1. ToF-SIMS

The positive ToF-SIMS spectrum obtained from the blue crystals is shown in Fig. 2. The positive ion spectrum of the blue crystals and that of the KI control are dominated by the K^+ ion. The comparison of the positive ToF-SIMS spectrum of the KI control with the blue crystals demonstrates that the $^{39}K^+$ peak of the blue crystals may saturate the detector and give rise to a peak that is atypical of the natural abundance of ^{41}K. The natural abundance of ^{41}K is 6.7%; whereas, the observed ^{41}K abundance from the blue crystals is 73%. The high-resolution mass assignment of the $m/z = 41$ peak of the blue crystals was consistent with ^{41}K, and no peak was observed at $m/z = 42.98$ ruling out $^{41}KH_2^+$. Moreover, the natural abundance of ^{41}K was observed in the positive ToF-SIMS spectra of $KHCO_3$, KNO_3, and KI standards that were obtained with an ion current such that the ^{39}K peak intensity was an order of magnitude higher than that given for the blue crystals. The saturation of the ^{39}K peak of the positive ToF-SIMS spectrum by the blue crystals is indicative of a unique crystalline matrix [11].

A small (50 counts) K^{2+} $m/z = 19.48$ ion was only observed in the positive ion spectrum of the blue crystals. Ga^+ $m/z = 69$, K_2^+ $m/z = 78$, $K(KCl^+$ $m/z = (113)$, I^+ $m/z = 127$, KI^+ $m/z = 166$, and a series of positive ions $K[KI]_n^+$ $m/z = (39 + 166n)$ are also observed.

The negative ion ToF-SIMS of the blue crystals shown in Fig. 3 was dominated by H^- and I^- peaks of about equal intensity. Iodide alone dominated the negative ion ToF-SIMS of the KI control. For both, O^- $m/z = 16$, OH^- $m/z = 17$, Cl^- $m/z = 35$, KI^- $m/z = 166$, a series of negative ions $I[KI]_n^-$ $m/z = (127 + 166n)$ are also observed.

The positive and negative ToF-SIMS spectrum obtained from the green crystals was similar to that obtained from the

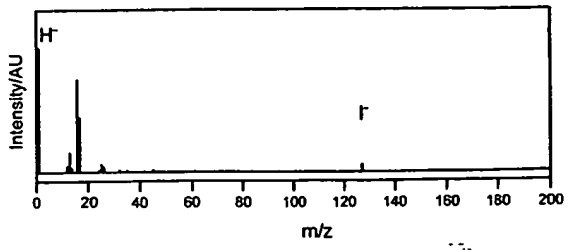

Fig. 4. The negative ToF-SIMS spectrum ($m/e = 0$–200) of the green crystals.

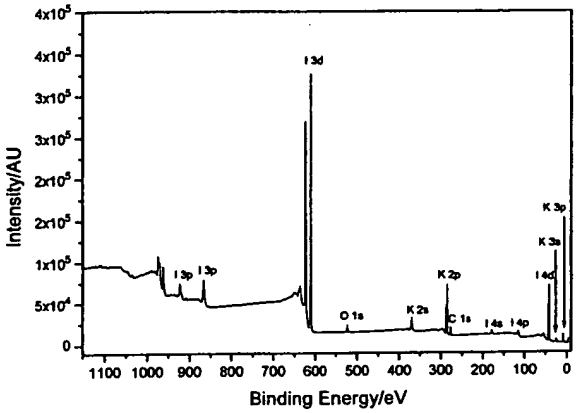

Fig. 5. The XPS survey scan of the blue crystals obtained on the Scienta instrument.

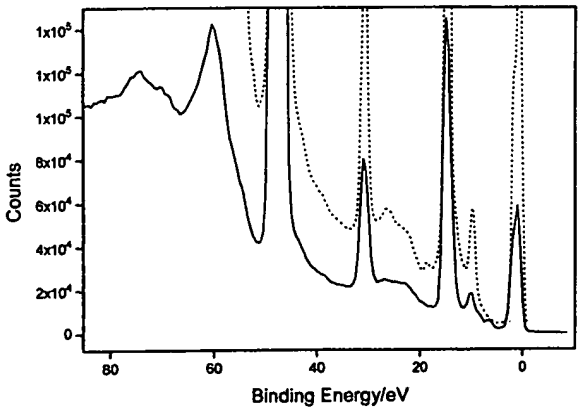

Fig. 6. The 0–85 eV binding energy region of a high-resolution XPS spectrum of the blue crystals (solid) and the control KI (dashed) obtained on the Scienta instrument.

Table 1
The results of the binding energies of selected core level electrons, full-width at half-maximum of the peaks, and energy of spin-orbit splitting for potassium iodo hydrides compared with KI

Compound	Peak	Binding energy (eV)	FWHM (eV)	S–O Splitting (eV)	Percentage (%)
KI	K $2p_{3/2}$	294.44	1.84	2.75	
	K $2p_{1/2}$	297.19	1.79		
	I $3d_{5/2}$	620.37	2.07	11.53	
	I $3d_{3/2}$	631.90	2.14		
Potassium iodo hydride	K $2p_{3/2}$	294.44	1.77	2.81	68.8
	K $2p_{1/2}$	297.21	1.69		
	K $2p_{3/2}$	292.90	1.76		
(Blue)	K $2p_{1/2}$	295.77	1.66	2.87	31.2
	I $3d_{5/2}$	621.01	2.19	11.52	
	I $3d_{3/2}$	632.53	2.30		
Potassium iodo hydride	K $2p_{3/2}$	294.37	1.83	2.77	58.3
	K $2p_{1/2}$	297.14	1.81		
	K $2p_{3/2}$	292.51	1.87		
(Green)	K $2p_{1/2}$	295.51	1.78	3.00	41.7
	I $3d_{5/2}$	621.08	2.17	11.52	
	I $3d_{3/2}$	632.60	2.20		

blue crystals except that the hydride ion peak of the negative ToF-SIMS spectrum obtained from the green crystals was much larger than that obtained from the blue crystals. The hydride peak of the green crystals was larger than the iodide peak as shown in Fig. 4; whereas, the hydride peak of the blue crystals was about equivalent to the iodide peak. These results are consistent with the formation of a higher hydride content or a higher hydride ion yield in the green crystals which may indicate that a higher binding energy hydride was formed by running the catalysis reaction at lower hydrogen pressure.

3.2. XPS

A survey spectrum was obtained over the region E_b = 0–1200 eV. The primary element peaks allowed for the determination of all of the elements present in the blue and green crystals and the control KI. The survey spectrum also detected shifts in the binding energies of the elements which had implications to the identity of the compound containing the elements.

The XPS survey scan of the blue crystals obtained on the Scienta instrument is shown in Fig. 5. The major species present in the blue crystals and the control are potassium and iodide. Small amounts of carbonate carbon and oxygen were also identified in the blue crystals. The K 3p and K 3s peaks of the blue crystals were shifted relative to those of the control KI. The K 3p and K 3s of the blue crystals occurred at 17 and 33 eV, respectively. The K 3p and K 3s of the control KI occurred at 17.5 and 33.5 eV, respectively. Hydrogen is the only element which does not have primary element peaks; thus, it is the only candidate to produce the shifted peaks.

No elements were present in the survey scan which could be assigned to peaks in the low binding energy region with the exception of the K 3p and K 3s peaks at 17 and 33 eV, respectively, the O 2s at 23 eV, and the I 5s, I $4d_{5/2}$, and I $4d_{3/2}$ peaks at 12.7, 51, and 53 eV, respectively. Accordingly, any other peaks in this region must be due to novel species. The 0–85 eV binding energy region of a high-resolution XPS spectrum of the blue crystals (solid) and the control KI (dashed) obtained on the Scienta instrument is shown in Fig. 6. The XPS spectrum of the blue crystals differs from that of KI by having additional features at 9.1 and 11.1 eV. The XPS peaks centered at 9.0 and 11.1 eV that do not correspond to any other primary element peaks may correspond to the $H^-(n=\frac{1}{4})$ $E_b=11.2$ eV hydride ion predicted by Mills [7] (Eq. (10)) in two different chemical environments where E_b is the predicted vacuum binding energy. In this case, the reaction to form $H^-(n=1/4)$ is given by Eqs. (3)–(5) and

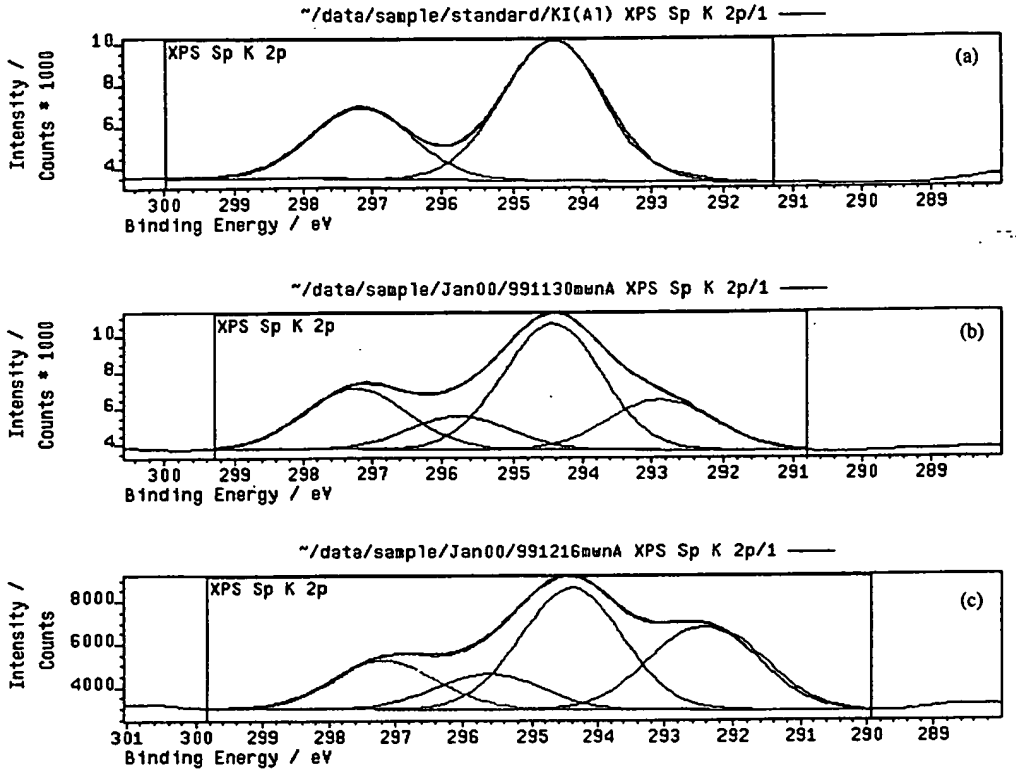

Fig. 7. (A) The XPS spectra of the K 2p core level in KI. (B) The XPS spectra of the K 2p core level in KHI (blue crystals). (C) The XPS spectra of the K 2p core level in KHI (green crystals).

Eq. (9). The hydride ion $H^-(n=\frac{1}{2})E_b = 3.05$ eV may also be present in the XPS of the blue crystals under the valence peak at about 3.5 eV. The reaction to form $H^-(n=\frac{1}{2})$ is given by Eqs. (6)–(8) and Eq. (9).

The binding energies and features of core level electrons of control KI and the blue and green crystals comprising the alkali halido hydride KHI were analyzed by XPS. Kratos XPS was used to investigate the local structure of KI and KHI by studying the metal core level K 2p electrons and the iodine core level I 3d electrons. As atomic hydrogen undergoes reaction with potassium catalyst to form a lower-energy hydrogen species which subsequently reacts with the potassium center in KI, alterations in the electronic structure of potassium such as changes in core level binding energies and spin-orbital energies relative to the starting compound, KI, are expected. The results of the determination of the binding energies of selected core level electrons, full-width at half-maximum of the peaks (FWHM), and energy of spin-orbital splitting for the blue and green crystal comprising KHI compared with KI are listed in Table 1, respectively. The XPS spectra of the K 2p core level in KI, KHI, (blue crystals) and KHI (green crystals) appear in Figs. 7A, 7B, and 7C respectively. The XPS spectra of the I 3d core level in KI, KHI (blue crystals), and KHI (green crystals) appear in Figs. 8A, 8B, and 8C, respectively.

In contrast to the K 2p core level, the I 3d core level FWHM in both compounds is very similar to KI. Comparing the alterations in the K core levels versus the I core level indicates that the lower-energy hydrogen species is bound to the metal center of KI. This binding influences the metal core level with little perturbation of the halogen core level.

Each of the spectra of potassium iodo hydride were curve fit with one spin-orbit splitting component having a similar FWHM and energy separation as that of the starting material potassium iodide. An additional spin-orbit splitting component had to be added to each potassium iodo hydride in order to obtain a good curve fit of the K 2p spectra. In each case, the second component of spin-orbit splitting is assigned to the formation of the alkali metal halido hydride, KHI. The presence of the novel hydride ion shifts the K 2p peaks to lower binding energies relative to the corresponding peaks of KI.

The XPS data clearly indicate a change in the electronic structure at the K core level and different bonding in KHI relative to that in the corresponding KI. It strongly suggests the formation of a novel metal hydride which is consistent with the supporting data provided by XPS given above and NMR, ToF-SIMS, and gas chromatography/mass spectroscopy given in the respective sections. The change in electronic structure is greatest with the green crystals which

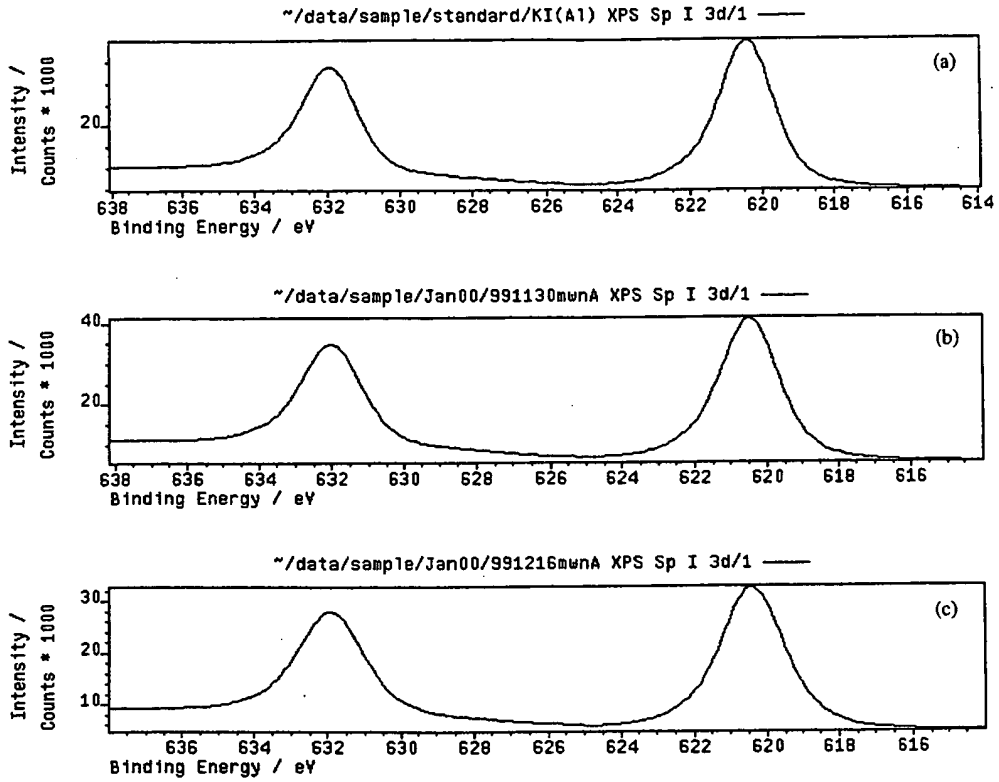

Fig. 8. (A) The XPS spectra of the I 3d core level in KI. (B) The XPS spectra of the I 3d core level in KHI (blue crystals). (C) The XPS spectra of the I 3d core level in KHI (green crystals).

indicates that a higher binding energy hydride is formed by running the catalysis reaction at lower hydrogen pressure.

The XPS survey scan of KI, the blue crystals, and the green crystals obtained on the Kratos instrument are shown in Figs. 9A–C, respectively. The 0–100 eV binding energy region of a high-resolution XPS spectrum of KI, the blue crystals, and the green crystals obtained on the Kratos instrument are shown in Figs. 10A–C, respectively. Peaks centered at 21 and 37 eV which do not correspond to any other primary element peaks were observed in the case of the green crystals. The intensity and shift match shifted K 3s and K 3p. Hydrogen is the only element which does not have primary element peaks; thus, it is the only candidate to produce the shifted peaks. These peaks may be shifted by a highly binding hydride ion $H^-(\frac{1}{6})$ with a binding energy of 22.8 eV given by Eq. (10) that bonds to potassium K 3p and shifts the peak to this energy. In this case, the K 3s is similarly shifted.

3.3. NMR

The ^{1}H MAS NMR spectra of the control KH and the blue crystals relative to external tetramethylsilane (TMS) are shown in Figs. 11 and 12, respectively. Three distinguishable resonances at 3.65, 0.13 and −0.26 ppm, respectively, were found in the NMR of KH. The broad 3.65 ppm peak of KH is assigned to KOH formed from air exposure during sample handling. The peaks at 0.13 and −0.26 ppm are assigned to hydride H.

Three distinguishable resonances at 0.081, −0.376 and −1.209 ppm, respectively, were found in the NMR of the blue crystals. A fourth very broad resonance may be present at −2.5 ppm. The peaks at 0.081 and −0.376 ppm are within the range of KH and may be ordinary hydride H in two different chemical environments that are distinct from those of the control KH. The resonances at −1.209 ppm and possibly at −2.5 ppm may be due to novel hydride ions.

The color of the blue crystals was found to change to white over 2 weeks of exposure to air. The color-fade rate was greatly increased upon grinding the blue crystal into a fine powder. A dynamic ^{1}H NMR study following the possible oxidation or hydrolysis of the blue crystals when exposed to air is shown in Figs. 13A–D. The ^{1}H MAS NMR spectra from ground blue crystals relative to external tetramethylsilane (TMS) following air exposure times of 1, 20, 40, and 60 mins are shown in Figs. 13A–D. Downfield ^{1}H resonances shifted gradually to 3.861 and 4.444 ppm and then to 5.789. Upfield resonances shifted to 1.157 ppm, as the exposure to

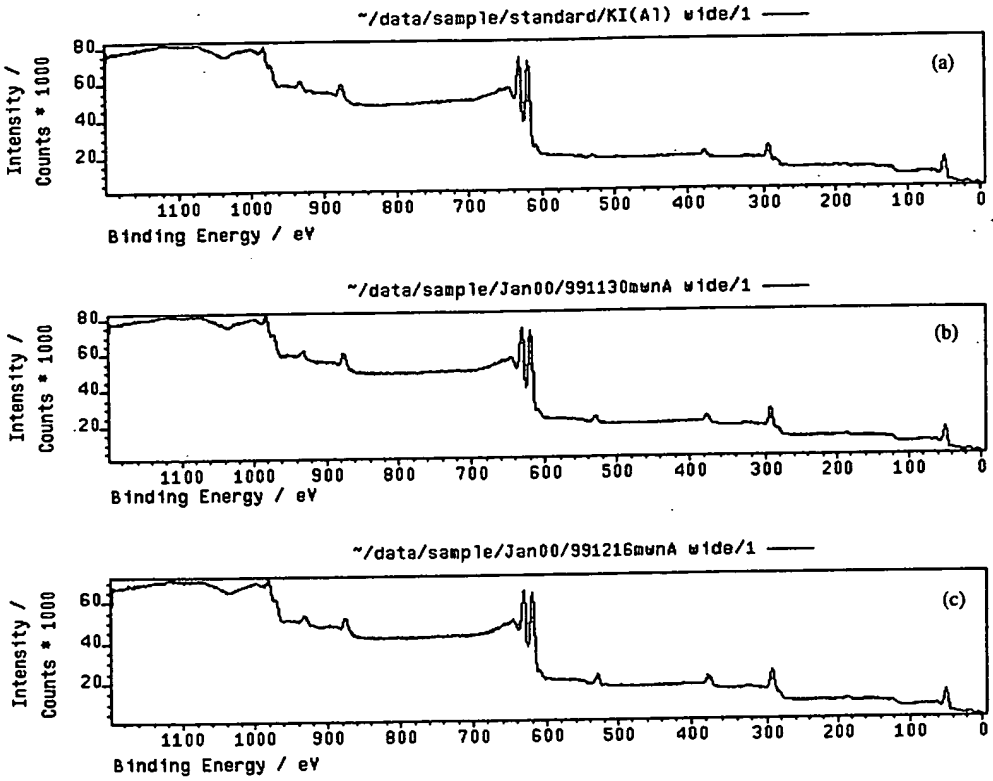

Fig. 9. (A) The XPS survey scan of KI obtained on the Kratos instrument. (B) The XPS survey scan of the blue crystals obtained on the Kratos instrument. (C) The XPS survey scan of the green crystals obtained on the Kratos instrument.

air was prolonged and the blue color concomitantly faded to white. The peak at 5.789 may be due to H of KOH in a chemical environment that is different from that of KOH formed by air exposure of KH. Since the downfield shift of the peak at 5.789 is substantially different from that observed for the control KH, 3.65 ppm, it may be due to KOH or a compound comprising KOH wherein H is increased binding energy hydrogen. The resonance at 1.157 comprises at least two peaks, one of which has a very broad upfield feature. These peaks may be novel hydride ions which are stable in air. In this case, the chemical environment is different from that of the blue crystals which showed potential novel hydride peaks at −1.209 ppm and possibly at −2.5 ppm. These observations strongly suggest that the H species in the blue crystals are new hydride species and may be responsible for the blue color. Decoupling studies are in progress to resolve the broad features of the blue crystal spectrum.

The ^{39}K MAS NMR spectra of KH, KI, and the blue crystals each showed a single resonance at 64.56, 52.71, and 53.32 ppm, respectively. The data indicate that the K local structure in the blue crystals is in between that of KI and KH.

To eliminate the possibility that KI influenced the local environment of the ordinary hydride of KH to produce an NMR resonance that was shifted upfield relative to KH alone, controls comprising KH and a KH/KI mixture were run. The ^{1}H MAS NMR spectra of the green crystals, the control comprising an equal molar mixture of KH and KI, and the control KH relative to external tetramethylsilane (TMS) are shown in Figs. 14A, 14B, and 14C, respectively. Ordinary hydride ion has a resonance at 1.1 and 0.8 ppm in the KH/KI mixture and in KH alone as shown in Figs. 14B and 14C, respectively. The additional peak at 4.5–4.6 ppm is assigned to KOH that formed by reaction of KH with air.

The presence of KI does not shift the resonance of ordinary hydride. The resonance at 1.1 ppm which is assigned to ordinary hydride ion was observed in the spectrum of the green crystals as shown in Fig. 14A. The 0.8 ppm resonance could not be resolved if it was present. A large distinct upfield resonance was observed at −2.5 ppm which was not observed in either control. This upfield shifted peak is consistent with a hydride ion with a smaller radius as compared with ordinary hydride since a smaller radius increases the shielding or diamagnetism. The −2.5 ppm peak is assigned to a novel hydride ion that has a smaller radius than that of the hydride ions observed in the case of the blue crystals since the upfield shift was larger in the case of the green crystals.

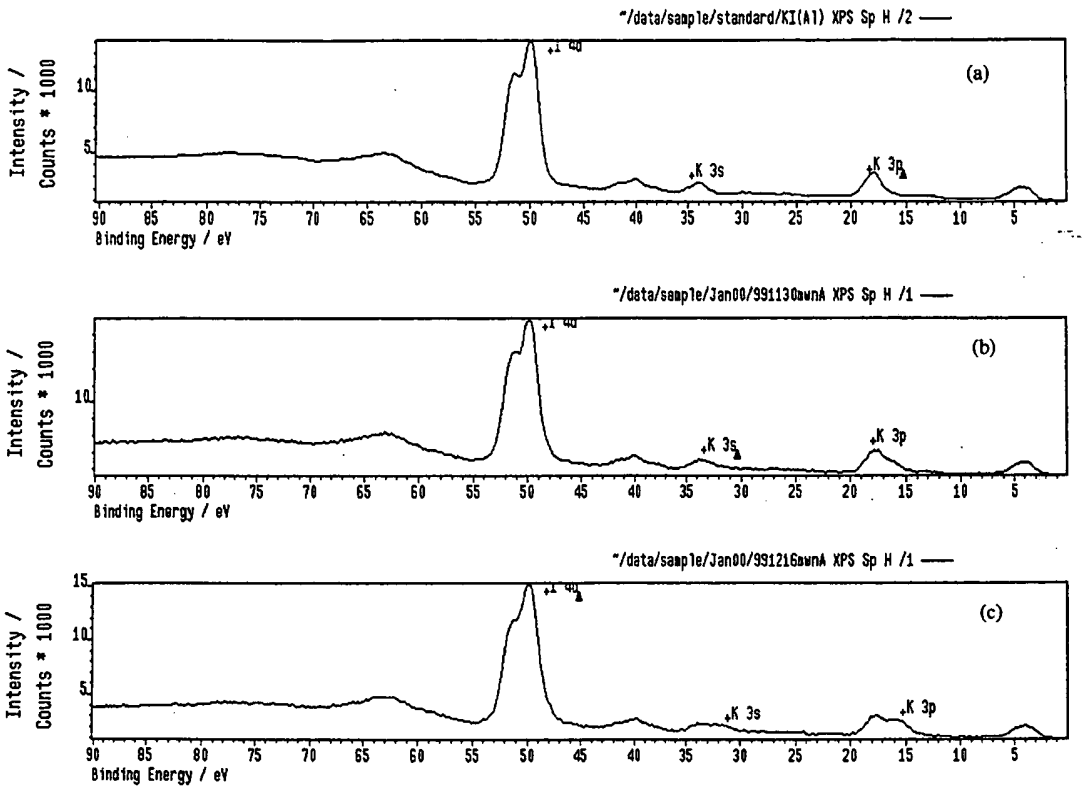

Fig. 10. (A) The 0–100 eV binding energy region of a high-resolution XPS spectrum of KI obtained on the Kratos instrument. (B) The 0–100 eV binding energy region of a high-resolution XPS spectrum of the blue crystals obtained on the Kratos instrument. (C) The 0–100 eV binding energy region of a high-resolution XPS spectrum of the green crystals obtained on the Kratos instrument.

3.4. FTIR

The FTIR spectra of KI (99.99%) was compared with that of the blue crystals. The FTIR spectra (45–3800/cm) of KI is given by Nyquist and Kagel [12]. The FTIR spectra (500–4000/cm) of the blue crystals is shown in Fig. 15. There are no vibrational bands in the 800–4000/cm region that can usually be assigned to covalent bondings. This eliminates the possibility of HI molecule embedded in KI crystals, since the H–I stretching mode is not observed at ~ 2309/cm. The FTIR spectra (500–1500/cm) of the blue crystals is shown in Fig. 16. Several bands shown in Fig. 16 such as 682, 712, 730/cm are found in the region assignable to ionic bonding or deformation vibration. The K–H vibrational band may be expected in this region. These bands are not present in pure KI. This implies that the compound of the blue crystals is ionic-like and contains different species from KI.

3.5. ESITOFMS

The positive ion ESITOFMS spectrum of the blue crystals and that of the KI control are dominated by the K^+ ion. A series of positive ions $K[KI]_n^+$ $m/z = (39 + 166n)$ were also observed. In addition, KHI^+ was only observed from the blue crystals.

3.6. LC/MS

No chromatographic peaks were observed of the selected ion monitoring LC/MS analysis of KI and sample solvent control.

Fig. 17A is the results of the selected ion monitoring LC/MS analysis of the blue crystals wherein the mass spectrum comprised the $m/z = 204.6$ ion signal. A chromatographic peak was observed at $RT = 22.45$ min. which corresponds to a nonpolar compound which gives rise to a $K(KI)^+$ mass fragment. The LC peak shown in Fig. 17A at $RT = 2.21$ min that comes out with the solvent front after injection corresponds to KI that gives rise to mass fragments K^+ and $K(KI)_x^+$.

Fig. 17B is the results of the Selected Ion Monitoring LC/MS analysis of the blue crystals wherein the mass spectrum comprised the m/z=370.6 ion signal. Chromatographic peaks were observed at $RT = 11.42$ and 23.38 min. which correspond to a nonpolar compounds having the $K(KI)_2^+$ mass spectrum fragment. The LC peak shown in Fig. 17B

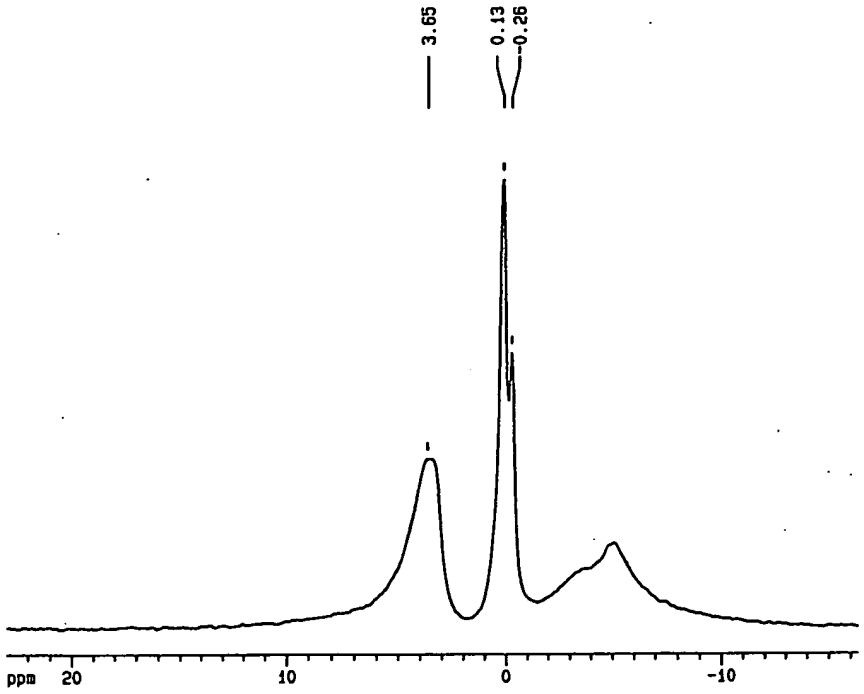

Fig. 11. The ^{1}H MAS NMR spectrum of the control KH relative to external tetramethylsilane (TMS).

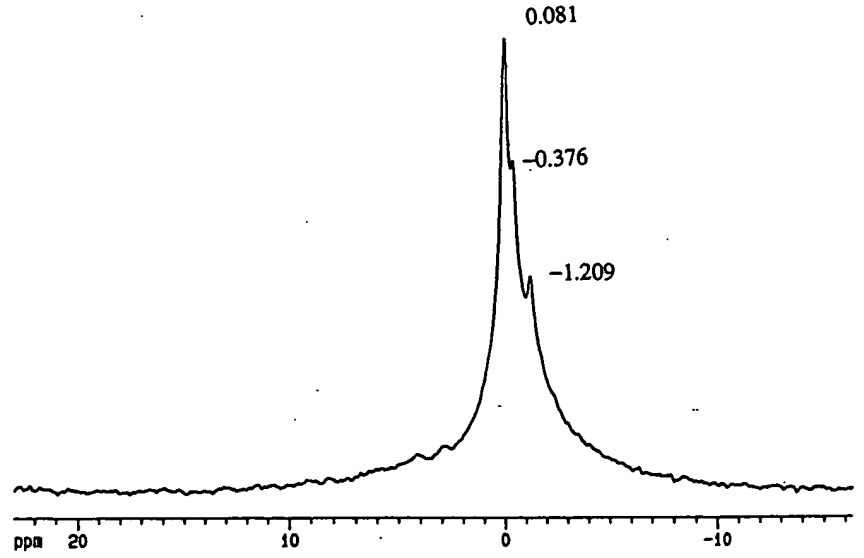

Fig. 12. The ^{1}H MAS NMR spectra of the blue crystals relative to external tetramethylsilane (TMS).

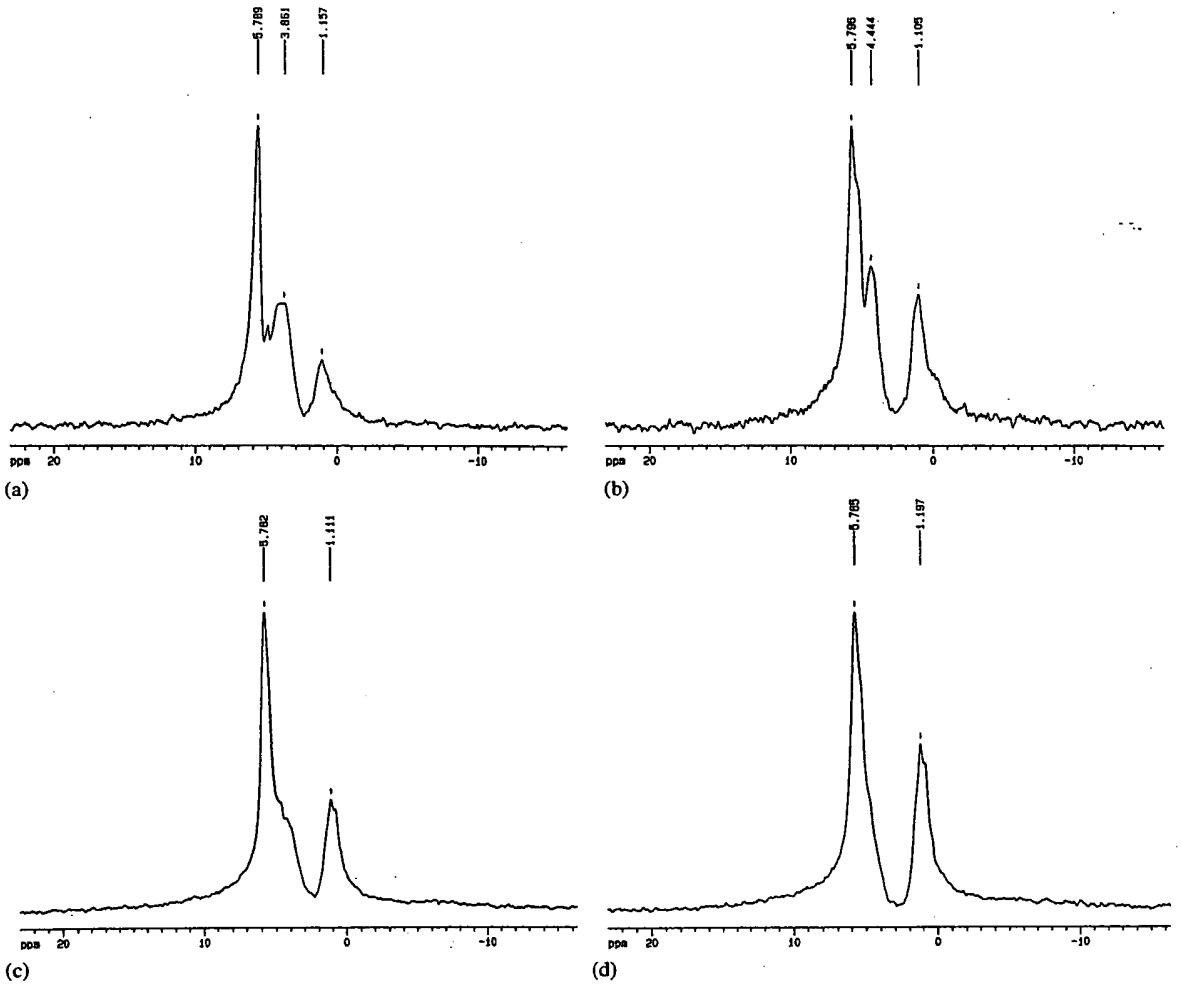

Fig. 13. (A) The ^{1}H NMR spectrum of the blue crystals exposed to air for 1 min. (B) The ^{1}H NMR spectrum of the blue crystals exposed to air for 20 min. (C) The ^{1}H NMR spectrum of the blue crystals exposed to air for 40 min. (D) The ^{1}H NMR spectrum of the blue crystals exposed to air for 60 min.

at $RT = 2.21$ min that comes out with the solvent front after injection corresponds to KI that gives rise to mass fragments K^+ and $K(KI)_x^+$.

The LC/MS data indicated that the blue crystal comprises a novel compound KHI which may contain two different hydride ions which gives rise to different mass fragmentation patterns. One KHI compound with a retention time of $RT = 11.42$ min may give rise to a $K(KI)_2^+$ mass fragment. Whereas, a second KHI compound with a retention time of about $RT = 23$ min may give rise to a $K(KI)^+$ and a $K(KI)_2^+$ mass fragment.

3.7. Gas chromatography

The gas chromatograph of the normal hydrogen gave the retention time for para hydrogen and ortho hydrogen as 22 and 24 min, respectively. Control KI and KI exposed to 500 mtorr of hydrogen at 600°C in the stainless-steel reactor for 48 h showed no hydrogen release upon heating to above 600°C with complete melting of the crystals. Dihydrino or hydrogen was released when the blue crystals were heated to above 600°C with melting which coincided with the loss of the dark blue color of these crystals.

The gas chromatograph of the dihydrino or hydrogen released from the blue crystals when the sample was heated to above 600°C with melting is shown in Fig. 18. The retention times drift with time due to conditioning of the column and absorption of contaminants. Thus, in previous studies [13], it was found that hydrogen must be present with dihydrino $H_2^*[n = \frac{1}{2}; 2c' = \sqrt{2}a_0/2]$ to identify the latter since the retention times are very close. But, these results confirm that the blue crystals are a hydride.

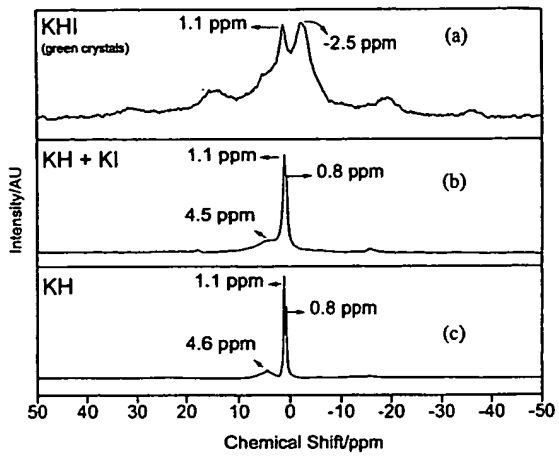

Fig. 14. (A) The ^{1}H MAS NMR spectrum of the green crystals relative to external tetramethylsilane (TMS). (B) The ^{1}H MAS NMR spectrum of the control comprising an equal molar mixture of KH and KI relative to external tetramethylsilane (TMS). (C) The ^{1}H MAS NMR spectrum of the control KH relative to external tetramethylsilane (TMS).

3.8. Mass spectroscopy

The dihydrino was identified by mass spectroscopy as a species with a mass to charge ratio of two ($m/e=2$) that has a higher ionization potential than that of normal hydrogen by recording the ion current as a function of the electron gun energy. The intensity as a function of time for masses $m/e = 1$, 2, and 3 obtained while changing the ionization potential (IP) of the mass spectrometer from 30 to 70 eV is shown for gas released from thermal decomposition of the blue crystals and ultrapure hydrogen in Figs. 19A and 19B, respectively. Upon increasing the ionization potential from 30 to 70 eV, typically the $m/e = 2$ ion current for the blue crystal sample increased by a factor of about 1000. Under the same pressure conditions, the $m/e=2$ ion current for the ultrapure hydrogen increased by a factor of less than 2.

The mass spectra ($m/e=0$–50) of the gases released from the thermal decomposition of the blue crystals at an ionization potential of 30 and 70 eV were recorded. As the ionization energy was increased from 30 to 70 eV $m/e = 4$ and 5 peaks were observed that was assigned to $H_4^+(\frac{1}{2})$ and $H_5^+(\frac{1}{2})$., respectively. No helium was observed by gas chromatography as given above in gas chromatography section. The peaks serve as a signatures for the presence of dihydrino molecules.

3.9. Elemental analysis

The quantitative elemental analysis showed that the blue crystal consisted of 0.5 wt% H, 22.58 wt% K and 75.40 wt% I, or in equivalent $KI_{1.028}H_{0.865}$.

4. Discussion

The elemental analysis and the positive and negative ToF-SIMS results of the blue crystals are consistent with the proposed structure KHI. In the former analysis, the hydrogen content was determined by combustion analysis which identifies ordinary hydride. The presence of novel hydride ions present in this sample may stabilize ordinary hydride. This is consistent with the NMR of this sample shown in Fig. 12 as compared with the NMR of ordinary hydride shown in Fig. 11. Furthermore, the NMR, XPS, and LC/MS data indicate that two forms of novel hydride were present. The known compounds KI and KH have the potassium ion in a +1 state. The compound KHI is unknown and extraordinary. The implied valence of potassium is +2. A K^{2+} peak was observed in the positive ToF-SIMS which supports +2 as the valence state. High-resolution solids probe magnetic sector mass spectroscopy is in progress to confirm this state. The preliminary results are positive.

Another unusual feature of the blue crystals is their intense dark blue color. The blue color was found to be dependent on the presence of H in KHI. The intensity of the dark blue color was directly related to the amount of hydrogen which was determined by thermal decomposition with quantification by gas chromatography. The presence of some $H^-(\frac{1}{2})$ is indicated by the thermal decomposition with the identification of a hydrogen-type molecule assigned to $H_2^*[2c' = a_0/\sqrt{2}]$ with an ionization potential of 62 eV (Eq. (13)). The presence of some $H^-(1/4)$ is indicated by the new XPS peak at about 11 eV.

Potassium metal may be embedded in KI crystals wherein potassium metal ionizes into K^+ and a free electron. This trapped free electron called an F-center may give rise to the blue color of the crystals. In contrast to other impurities such as OH^-, the presence of ordinary hydrogen has a small influence on the emission lifetime of an F center in a similar alkali halide, KCl, which corresponds to a slight decrease in the coloration of F-centers by radiationless relaxation [14].

Coloration may occur by exposure of an alkali halide to alkali metal vapor at high temperature followed by thermal quenching. A nonhydrogen control was run under identical conditions used to synthesize the blue crystals except that helium replaced hydrogen. The resulting crystals appeared dirty brown with minimal coloring and contained inclusions of colloidal alkali metal.

An explanation of the absolutely reproducible homogeneous very dark blue coloration is required. Two mechanisms may explain the results. The catalysis of hydrogen creates an intense hydrogen plasma [1–6]. The predominant mechanism of forming F centers is by applying ionizing radiation. Thus, the extreme ultraviolet (EUV) radiation from the catalysis with the production of the hydrino hydride ions may be the source of F centers. In this case, the hydride content correlates with the color because the EUV emission corresponds to hydride production. Or, the hydrino hydride

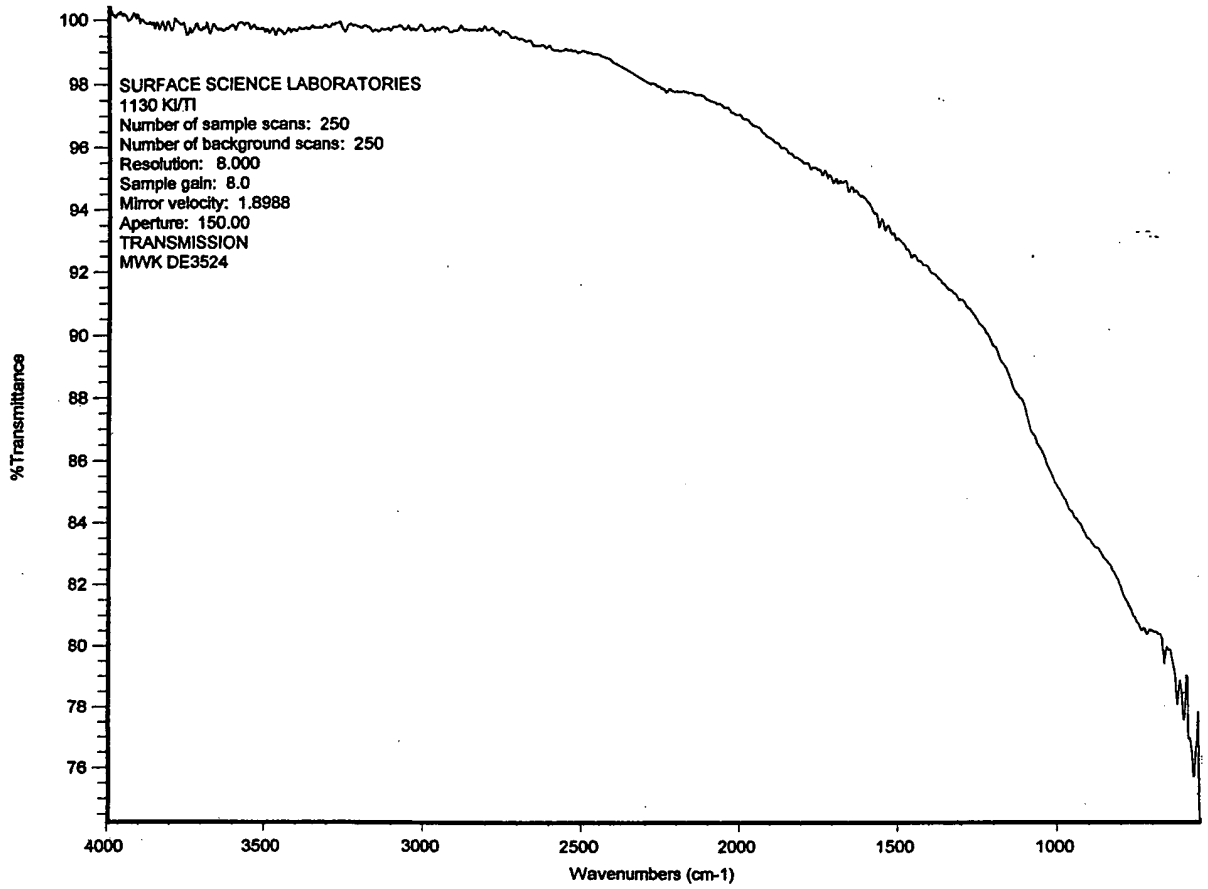

Fig. 15. The FTIR spectra (500–4000/cm) of the blue crystals.

ion assists in the formation, stability, or emission efficiency of F centers. To determine if the former explanation has merit, experiments are in progress whereby EUV emission of the gas cell reactor is correlated with the intensity of coloration of the blue crystalline product as determined by visible spectroscopy. To determine whether the latter explanation has merit, Raman spectroscopy experiments such as those of Gustin et al. [14] of the relaxation mechanism of excited F centers of the blue crystals are planned.

When the blue crystals were pulverized or exposed to air for a prolong period of about two weeks the blue color faded and white crystals formed. Investigations of these white crystals are in progress. Preliminary data indicate a hydride containing carbon dioxide, oxygen, and water-derived species. For example, the positive ToF-SIMS of the air-exposed crystals contained three new series of positive ions: $\{K[KH\ KHCO_3]_n^+\ m/z = (39 + 140n)$, $K_2OH[KH\ KHCO_3]_n^+\ m/z = (95 + 140n)$, and $K_3O[KH\ KHCO_3]_n^+\ m/z = (133 + 140n)\}$. These ions correspond to inorganic clusters containing novel hydride combinations (i.e. KH $KHCO_3$ units plus other positive fragments). The negative ion spectrum was dominated by O^- and OH^- peaks as well as H^- and I^- peaks. A $KHIO^-$ peak was present only in the negative spectrum of the air-exposed blue crystals and not in the spectrum of air-exposed KI control. The formation of the novel compound potassium hydride potassium hydrogen carbonate comprising $H^-(\frac{1}{2})$ and $H^-(\frac{1}{4})$ is consistent with the changes in the NMR observed with air exposure of the blue crystals. KH $KHCO_3$ has been made in an electrolytic cell reactor wherein potassium ions served as the catalysts according to Eqs. (6)–(8) [15]. KH $KHCO_3$ has also been synthesized in a gas cell energy reactor wherein potassium ions served as the catalyst according to Eqs. (3)–(5) [16,17].

An explanation for the color of the green crystals may be a charge transfer transition due to the presence of a K^{2+} in the crystal which is stabilized by a higher binding energy hydride ion relative to the blue crystals. The ToF-SIMS, XPS, and NMR results support this explanation.

The hydride peak of the green crystals was larger than the iodide peak; whereas, the hydride peak of the blue crystals was about equivalent to the iodide peak. These results are consistent with the formation of a higher hydride content or a higher hydride ion yield in the green crystals which may

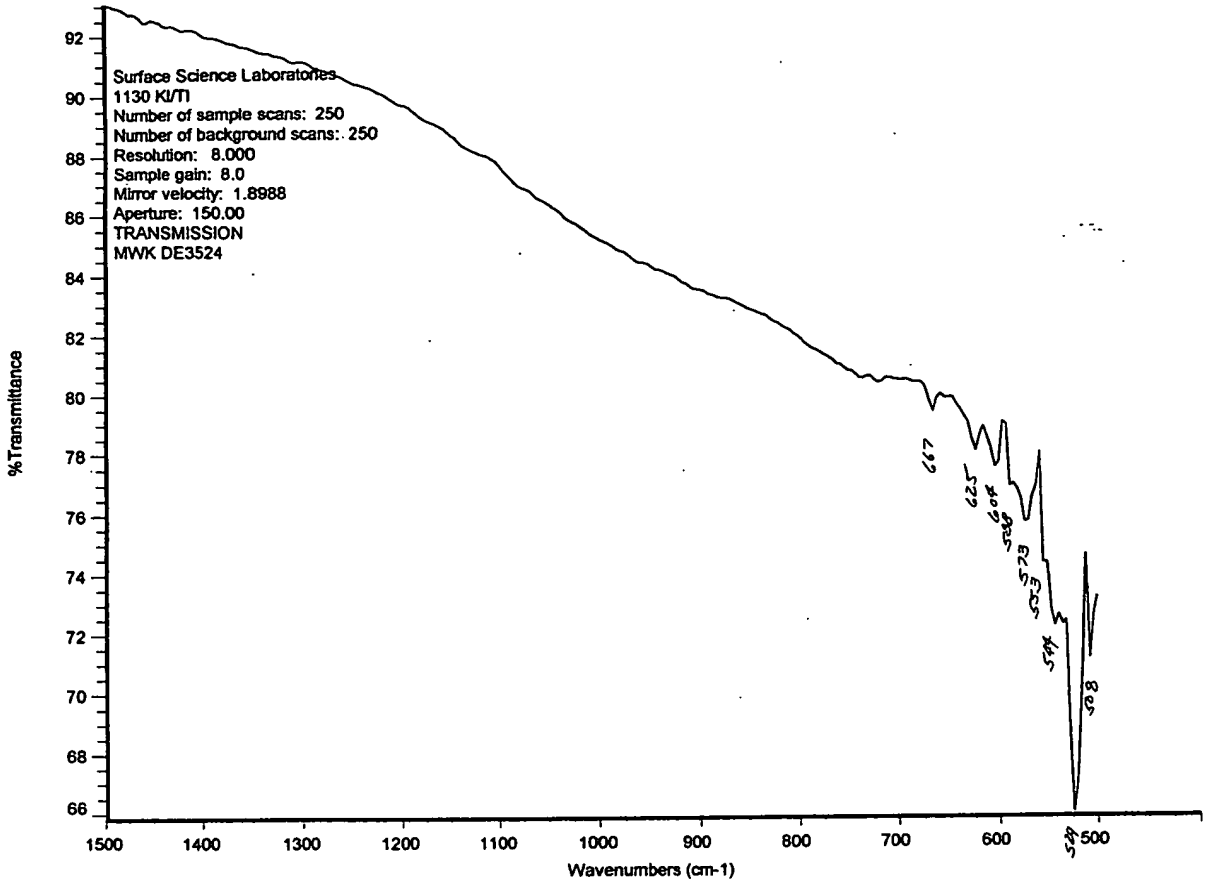

Fig. 16. The FTIR spectra (500–1500/cm) of the blue crystals.

indicate that a higher binding energy hydride was present in the green crystals.

The XPS data of the core levels clearly indicate a change in the electronic structure and different bonding in KHI relative to that in the corresponding KI. This binding influences the metal core level with little perturbation of the halogen core level. Comparing the alterations in the K core levels versus the I core level indicates that the lower-energy hydrogen species binds to the metal center of KI. An additional spin-orbit splitting component had to be added to each potassium iodo hydride in order to obtain a good curve fit of the K 2p spectra. In each case, the second component of spin-orbit splitting is assigned to the formation of the alkali metal halido hydride, KHI. The presence of the novel hydride ion shifts the K 2p peaks to lower binding energies relative to the corresponding peaks of KI. It strongly suggests the formation of a novel metal hydride which is consistent with the supporting data provided by XPS given above and NMR, ToF-SIMS, and gas chromatography/mass spectroscopy given in the respective sections. The change in electronic structure is greatest with the green crystals which indicates that a higher binding energy hydride is formed by running the catalysis reaction at lower hydrogen pressure.

The 0–100 eV binding energy region of a high-resolution XPS spectra of the blue and green crystals indicate the presence of the hydride ions $H^-(\frac{1}{2})$ and $H^-(\frac{1}{4})$ in the case of the blue crystals and the presence of the higher binding energy hydride ion $H^-(\frac{1}{6})$ in the case of the green crystals.

The upfield peak in the NMR spectrum of the green crystals at −2.5 ppm was assigned to a novel hydride ion that has a smaller radius than that of the hydride ions observed in the case of the blue crystals corresponding to resonances at −0.376 and −1.209 ppm since the upfield shift was larger in the case of the green crystals. A smaller radius corresponds to a higher binding energy.

5. Conclusions

The ToF-SIMS, XPS, NMR, FTIR, ESITOFMS, LC/MS, thermal decomposition with analysis by GC, and MS, and

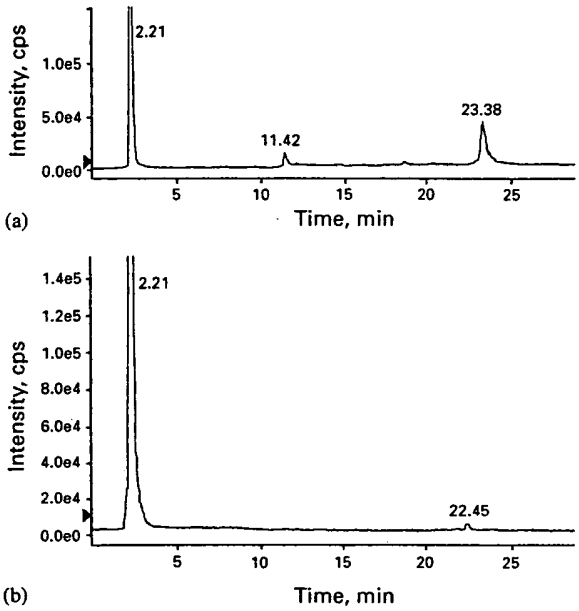

Fig. 17. (A) The results of the selected ion monitoring LC/MS analysis of the blue crystals wherein the mass spectrum comprised the $m/z = 204.6$ ion signal. (B) The results of the selected ion monitoring LC/MS analysis of the blue crystals wherein the mass spectrum comprised the $m/z = 370.6$ ion signal.

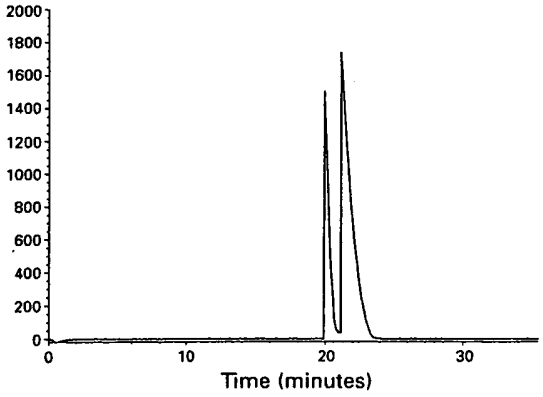

Fig. 18. The gas chromatograph of the dihydrino or hydrogen released from the blue crystals when the sample was heated to above 600°C with melting.

elemental analysis results confirm the identification of KHI having hydride ions, $H^-(\frac{1}{2})$, $H^-(\frac{1}{4})$, and $H^-(\frac{1}{6})$. Two forms of hydride ion ($H^-(\frac{1}{2})$ and $H^-(\frac{1}{4})$) may be formed according to Eqs. (5), (8), and (9) which is supported by the XPS, NMR, and LC/MS data of the blue crystals. The thermal decomposition with mass spectroscopic analysis indicates that at least $H^-(\frac{1}{2})$ is present in KHI of the blue crystals.

The ToF-SIMS results of a more intense hydride peak, the NMR results of a greater upfield shifted peak, and the XPS results that the change in electronic structure was greatest with the green crystals relative to the blue crystals indicate that a higher binding energy hydride was formed by running the catalysis reaction at lower hydrogen pressure. The XPS results of the low binding energy region are consistent with the presence of $H^-(\frac{1}{6})$ in the green crystals. This product is predicted by an autocatalysis reaction of two $H(\frac{1}{4})$ atoms which has been confirmed by extreme ultraviolet spectroscopy [3].

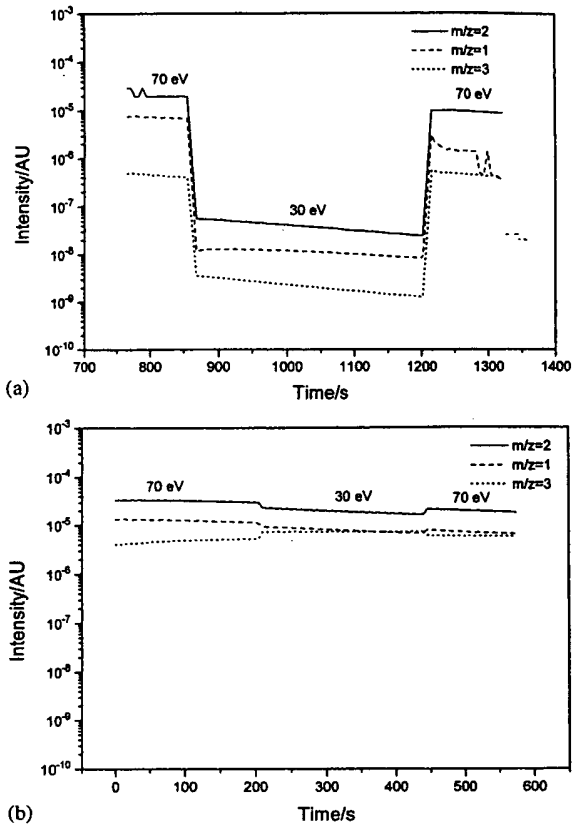

Fig. 19. (A) The intensity as a function of time for masses $m/e = 1$, 2, and 3 obtained while changing the ionization potential (IP) of the mass spectrometer from 30 to 70 eV for gas released from thermal decomposition of the blue crystals. (B) The intensity as a function of time for masses $m/e = 1$, 2, and 3 obtained while changing the ionization potential (IP) of the mass spectrometer from 30 to 70 eV for ultrapure hydrogen.

The chemical structure and properties of KHI having a hydride ion with a high binding energy are indicative of a new field of hydride chemistry. The novel hydride ion may combine with other cations such as other alkali cations and alkaline earth, rare earth, and transition element cations. Numerous novel compounds may be synthesized with extraordinary properties relative to the corresponding compounds having ordinary hydride ions [15–19]. These novel compounds may have a breath of applications.

References

[1] Mills R, Dong J, Lu Y. Observation of extreme ultraviolet hydrogen emission from incandescently heated hydrogen gas with certain catalysts. 1999 Pacific Conference on Chemistry and Spectroscopy and the 35th ACS Western Regional Meeting, Ontario Convention Center, California, October 6–8, 1999.

[2] Mills R, Dong J, Lu Y. Observation of extreme ultraviolet hydrogen emission from incandescently heated hydrogen gas with certain catalysts. Int J Hydrogen Energy, 2000;25: 919–43.

[3] Mills R. Observation of extreme ultraviolet hydrogen and hydrino emission from hydrogen-KI plasmas produced by a hollow cathode discharge. Int J Hydrogen Energy, submitted.

[4] Mills R. Temporal behavior of light-emission in the visible spectral range from a Ti-K2CO3-H-Cell. Int J Hydrogen Energy, in press.

[5] Mills R, Lu Y, Onuma T. Formation of a hydrogen plasma from an incandescently heated hydrogen-potassium gas mixture and plasma decay upon removal of heater power. Int J Hydrogen Energy, submitted.

[6] Mills R, Nansteel M, Lu Y. Observation of extreme ultraviolet hydrogen emission from incandescently heated hydrogen gas with strontium that produced an optically measured power balance that was 4000 times the control. Int J Hydrogen Energy, in press.

[7] Mills R. The grand unified theory of classical quantum mechanics, January 2000 ed. Cranbury, New Jersey: BlackLight Power, Inc., Distributed by Amazon.com.

[8] Linde DR. CRC handbook of chemistry and physics, 78th ed. Boca Raton, FL: CRC Press, 1997. p. 10-214–10-216.

[9] Microsc Microanal Microstruct 1992;3:1.

[10] For recent specifications see PHI Trift II, ToF-SIMS Technical Brochure, Eden Prairie, MN 55344, 1999.

[11] Briggs D, Seah MP. editors. Ion and neutral spectroscopy. In Practical surface analysis, vol. 2. 2nd ed. New York: Wiley, 1992.

[12] Nyquist RA, Kagel RO. Infrared spectra of inorganic compounds. New York: Academic Press, 1971. p. 464–5.

[13] Mills R. NOVEL HYDRIDE COMPOUNDS. PCT US98/14029 filed on July 7, 1998.

[14] E. Gustin, M. Leblans, A. Bouwen, D. Shoemaker, Phys Rev B 49 (2) (1994) 916–26.

[15] R. Mills, Novel inorganic hydride, Int J Hydrogen Energy 25 (2000) 669–83.

[16] Mills R, He J, Dhandapani B. Novel hydrogen compounds. 1999 Pacific Conference on Chemistry and Spectroscopy and the 35th ACS Western Regional Meeting, Ontario Convention Center, California, October 6–8, 1999.

[17] Mills R, Dhandapani B, Nansteel M, He J. Synthesis and characterization of novel hydride compounds. Int J Hydrogen Energy, in press.

[18] R. Mills, Novel hydrogen compounds from a potassium carbonate electrolytic cell, Fusion Technol 37 (2) (2000) 157–82.

[19] Mills R. Highly stable novel inorganic hydrides. Int J Inorganic Mater., submitted.